Clim. Past Discuss., doi:10.5194/cp-2016-59, 2016
Manuscript under review for journal Clim. Past
Published: 20 June 2016

Climate of the Past Discussions
Open Access
EGU

Glacial $\delta^{13}C$ decreases in the western South Atlantic forced by millennial changes in Southern Ocean ventilation

Marília C. Campos[1], Cristiano M. Chiessi[1], Ines Voigt[2], Alberto R. Piola[3,4], Henning Kuhnert[2], Stefan Mulitza[2]

[1]School of Arts, Sciences and Humanities, University of São Paulo, São Paulo, 03828-000, Brazil
[2]MARUM – Center for Marine Environmental Sciences, University of Bremen, Bremen, 28359, Germany
[3]Servicio de Hidrografia Naval (SHN), Buenos Aires, C1270ABV, Argentina
[4]Dept. Ciencias de la Atmósfera y los Océanos, FCEN, Universidad de Buenos Aires, C1428 EHA, and Instituto Franco–Argentino sobre Estudios de Clima y sus Impactos, CNRS/CONICET, C1428EGA, Argentina

Correspondence to: Marília C. Campos (marilia.carvalho.campos@usp.br)

Abstract. Abrupt millennial–scale climate change events of the last deglaciation (i.e., Heinrich Stadial 1 and the Younger Dryas) were accompanied by marked increases in atmospheric CO_2 presumably originated by outgassing from the Southern Ocean. However, information on the preceding Heinrich Stadials during the last glacial period is scarce. Here we present stable carbon isotopic data ($\delta^{13}C$) from two species of planktonic foraminifera from the western South Atlantic that reveal major decreases (up to 1‰) during Heinrich Stadials 3 and 2. These $\delta^{13}C$ decreases are most likely related to millennial–scale periods of intensification in Southern Ocean deep water ventilation presumably associated with a weak Atlantic meridional overturning circulation. After reaching the upper water column of the Southern Ocean, the $\delta^{13}C$ depletion would be transferred equatorward via central and thermocline waters. Together with other lines of evidence, our data are consistent with the hypothesis that the CO_2 added to the atmosphere during abrupt millennial–scale climate change events during the last glacial period also originated in the ocean and reached the atmosphere by outgassing from the Southern Ocean. The temporal evolution of $\delta^{13}C$ during Heinrich Stadials in our records is characterized by two relative minima separated by a relative maximum. This "w–structure" is also found in North Atlantic and South American records, giving us confidence that such structure is a pervasive feature of Heinrich Stadial 2 and, possibly, also Heinrich Stadial 3.

Keywords: Planktonic Foraminifera. Stable Carbon Isotopes. Heinrich Stadials. Southern Ocean.

1 Introduction

Heinrich Stadials (HSs) are abrupt millennial–scale climate change events marked by an anti-phase interhemispheric temperature pattern which is usually termed the bipolar seesaw (Broecker, 1998). One widely accepted mechanism for the bipolar seesaw is related to changes in the strength of the Atlantic meridional overturning circulation (AMOC), likely caused by fresh water input into the high latitudes of the North Atlantic (Mix et al., 1986; Crowley, 1992; Stocker, 1998). During HSs, a weak AMOC occurred simultaneously to cooling in the high latitudes of the surface North Atlantic (Sachs and

Clim. Past Discuss., doi:10.5194/cp-2016-59, 2016
Manuscript under review for journal Clim. Past
Published: 20 June 2016

Lehman, 1999; Bard et al., 2000), warming of the surface South Atlantic (Barker et al., 2009; Chiessi et al., 2015), a southward migration of the Intertropical Convergence Zone (ITCZ) (Arz et al., 1998; Deplazes et al., 2013), strengthening of the South American monsoon system (SAMS) (Cruz et al., 2006; Kanner et al., 2012), and an increase in atmospheric CO_2 (CO_{2atm}) (Ahn and Brook, 2008; Ahn and Brook, 2014). It has been suggested that the origin of the CO_{2atm} rise was ocean–sourced (Anderson et al., 2009; Denton et al., 2010; Mariotti et al., 2016). The occurrence of stable carbon isotope ($\delta^{13}C$) minima during HS1 (last deglaciation) in planktonic foraminiferal records from the Indo–Pacific Ocean, Southern Ocean, and South Atlantic Ocean (Oppo and Fairbanks, 1989; Ninnemann and Charles, 1997; Mulitza et al., 1999; Spero and Lea, 2002) suggests that the signal should have originated from the ocean region most directly connected to all major oceanic basins, i.e., the Southern Ocean (Ninnemann and Charles, 1997). Under a weak AMOC, wind–driven upwelling of the Circumpolar Deep Water (CDW) in the Southern Ocean would become stronger, breaking up the stratification of the Southern Ocean, and enhance outgassing of CO_2 to the atmosphere (Anderson et al., 2009; Denton et al., 2010). The CDW forms from mixing of North Atlantic Deep Water (NADW), Indian Deep Water (IDW) and Pacific Deep Water (PDW) and upwells to the south of the Antarctic Polar Front driven by the prevailing westerly winds (Marshall and Speer, 2012). Therefore, the $\delta^{13}C$ signal of CDW (ca. 0.4‰) (Kroopnick, 1985) lies between that of NADW (ca. 1‰) (Kroopnick, 1985) and IDW/PDW (ca. 0.2 to -0.2‰) (Kroopnick, 1985) (Oppo and Fairbanks, 1987; Charles and Fairbanks, 1992). During periods of weak AMOC the influence of NADW on the Southern Ocean is reduced (Charles and Fairbanks, 1992), and the $\delta^{13}C$ of CDW should decrease since this water mass would have a relatively larger contribution from low–$\delta^{13}C$ IDW and PDW. Thus, the strengthening in the Southern Ocean upwelling would bring old, respired ^{13}C–depleted waters to the surface that would then be transferred equatorward via central and thermocline waters (Spero and Lea, 2002). This mechanism (i.e., a weak AMOC leading to a strengthening of the Southern Ocean upwelling, a $\delta^{13}C$ depletion and an increased outgassing of CO_2 to the atmosphere) may be a common feature of HSs (Anderson et al., 2009) but, so far, planktonic foraminiferal $\delta^{13}C$ records corroborating this process are mostly available for abrupt millennial–scale climate change events of the last deglaciation while information of the last glacial period is still scarce.

Here we addresses this issue for HS3 and HS2 using planktonic foraminiferal (*Globigerinoides ruber* white (*G. ruber* w) and *Globorotalia inflata* (*G. inflata*)) $\delta^{13}C$ data from a high temporal resolution marine sediment core (GeoB6212-1), collected near 32° S off south–eastern South America (SESA). Our data suggest that HS3 and HS2 were marked by significant $\delta^{13}C$ decreases in upper water column most likely caused by millennial–scale strengthening of Southern Ocean upwelling.

2 Regional setting

The upper water column of the study area is dominated by the southward flowing Brazil Current (BC), the western branch of the South Atlantic subtropical gyre. The BC is one of the weakest western boundary currents in the world ocean (Peterson and Stramma, 1991) carrying warm, saline and nutrient–depleted subtropical waters southward (Olson et al., 1988). The BC originates near 10-15° S from the bifurcation of the Southern South Equatorial Current as it approaches the western slope of

Clim. Past Discuss., doi:10.5194/cp-2016-59, 2016
Manuscript under review for journal Clim. Past
Published: 20 June 2016

the Brazil Basin (Stramma et al., 1990; Peterson and Stramma, 1991). Around 38° S the BC encounters the northward flowing Malvinas Current (MC) (i.e., Brazil/Malvinas Confluence), where the opposing flows turn south–east and flow offshore. The offshore region is characterized by intense mesoscale variability. After collision and considerable mixing the warm–salty BC fractions flow eastward as the South Atlantic Current (Olson et al., 1988; Peterson and Stramma, 1991), while the majority of the cold fresh MC waters veer southeastward to rejoin the Antarctic Circumpolar Current.

The BC transports Tropical Water (TW) and South Atlantic Central Water (SACW). TW occupies the mixed layer, i.e., the upper ca. 100 m of the water column, with a mean temperature of 20 °C and mean salinity of 36 psu (Tsuchiya et al., 1994). TW originates in the tropics-subtropics transition region by subduction, creating a subsurface salinity maximum capping the central waters (Memery et al., 2000; Tomczak and Godfrey, 2003) (Fig. 1). SACW occupies the permanent thermocline from ca. 100 to 500 m water depth. Its temperature ranges from 6 to 20 °C and its salinity spans from 34.6 to 36 psu (Memery et al., 2000). Two types of SACW have been identified (Stramma et al., 2003). The low–density type of SACW which is mainly found in the South Atlantic subtropical gyre is formed by subduction of a low–density type of Subantarctic Mode Water (SAMW) along the southern edge of the gyre (Gordon, 1981; Stramma and England, 1999). A denser variety of SACW originates in the South Indian Ocean and is brought into the South Atlantic by the Agulhas Current (Sprintall and Tomczak, 1993) (Fig. 1).

Just below the permanent thermocline, Antarctic Intermediate Water (AAIW) occupies the water column from ca. 500 to 1200 m water depth (Stramma and England, 1999). AAIW is characterized as a cold and low salinity water mass (Piola and Georgi, 1982; Tomczak and Godfrey, 2003). Around the southern tip of South America, AAIW originates by subduction of cold and fresh Antarctic Surface Water across the Antarctic Polar Front, and by contribution of a dense type of SAMW that originates from deep winter convection in the Subantarctic Zone (Molinelli, 1981; Naveira Garabato et al., 2009). AAIW is advected eastward through the Drake Passage by the Antarctic Circumpolar Current and turns northwards with the MC into the South Atlantic (Piola and Gordon, 1989). Since AAIW circulation follows the anticyclonic flow of the subtropical gyre the majority of the northward flow occurs in the eastern basin (McCartney, 1977; Stramma and England, 1999; Tomczak and Godfrey, 2003). However, intense mixing in the Brazil/Malvinas Confluence also leads to direct northward influence in the western South Atlantic that can, to some extent , influences the formation region of SACW (e.g., Piola and Georgi, 1982) (Fig. 1 and 2).

In the modern South Atlantic, the distribution of dissolved inorganic carbon $\delta^{13}C$ ($\delta^{13}C_{DIC}$) allows the identification of its major water masses. TW and SACW show high $\delta^{13}C_{DIC}$ values of ca. 2‰. AAIW presents $\delta^{13}C_{DIC}$ values of ca. 0.7‰. NADW derives from the North Atlantic and shows $\delta^{13}C_{DIC}$ values of ca. 1‰. The NADW layer is surrounded by Upper and Lower CDW which present $\delta^{13}C_{DIC}$ values of ca. 0.4‰ (Kroopnick, 1985). Since planktonic foraminiferal $\delta^{13}C$ reflects the $\delta^{13}C_{DIC}$ of the ambient seawater, we use it as a proxy for the past oceanic carbon system (Mulitza et al., 1999; Spero, 1992).

Changes in upper ocean properties and circulation patterns are also closely associated with changes in the atmospheric circulation. Positive sea surface temperature (SST) anomalies in the western South Atlantic, likely associated to changes in

Clim. Past Discuss., doi:10.5194/cp-2016-59, 2016
Manuscript under review for journal Clim. Past
Published: 20 June 2016

the strength of the AMOC (Knight et al., 2005), have been correlated with positive anomalies in the strength of the SAMS and, consequently, with the increase of precipitation over SESA (Chaves and Nobre, 2004). The SAMS and its main components – the ITCZ, the South Atlantic Convergence Zone (SACZ), and the South American Low Level Jet (SALLJ) – are the main atmospheric drivers of the hydroclimate of tropical and subtropical SESA to the east of the Andes (Garreaud et al., 2009). The ITCZ is a global convective belt in the equatorial region, and the SACZ is an elongate NW-SE convective belt that originates in the Amazon Basin and extends southeastward above the northern portion of SESA and the adjacent subtropical South Atlantic. The SALLJ is a NW-SE humidity flux from the west Amazon Basin to the subtropical region of SESA (Zhou and Lau, 1998; Carvalho et al., 2004; Schneider et al., 2014). This southward water vapour flux is a crucial source of precipitation to the Plata River drainage basin (Berbery and Barros, 2002), which is a source of continental borne sediments to our core site.

3 Materials and methods

3.1 Marine sediment core

We investigated sediment core GeoB6212-1 (32.41° S, 50.06° W, 1010 m water depth, 790 cm core length) (Schulz et al., 2001) collected from the continental slope off SEAS where the upper water column is under the influence of the BC, and thus the TW and SACW (Fig. 1). This gravity core was raised at the Rio Grande Cone, a major sedimentary feature in the western Argentine Basin. As our focuses here are HS3 and HS2, we analysed a section from the bottom of the core (768 cm core depth; ca. 33 cal ka BP) up to 290 cm core depth (ca. 20 cal ka BP). Visual core inspection provided evidence for the presence of sand lenses at 330 and 368 cm core depth (Schulz et al., 2001; Wefer et al., 2001). Therefore we did not sample these depths. The section of interest of GeoB6212-1 was sampled every 2.5 cm with syringes of 10 cm^3. All samples were wet sieved, oven–dried at 50 °C and the fraction larger than 150 μm was stored in glass vials for subsequent analyses.

3.2 Age model

The age model of core GeoB6212-1 is based on 14 AMS radiocarbon ages from planktonic foraminifera (Table 1, Fig. 3). For each sample, we hand–picked under a binocular microscope around 10 mg of planktonic foraminifera shells from the sediment fraction larger than 150 μm. Samples were analysed at the Poznan Radiocarbon Laboratory, Poland, and at the Beta Analytic Radiocarbon Dating Laboratory, USA (Table 1). All radiocarbon ages were calibrated with the calibration curve IntCal13 (Reimer et al., 2013) with the software Bacon 2.2 (Blaauw and Christen, 2011). A marine reservoir correction of 400 years was applied (Bard, 1988). All ages are reported as calibrated years before present (cal a BP; present is 1950 AD). To construct the age model we used Bayesian statistics in the software Bacon 2.2 (Blaauw and Christen, 2011). Default parameter settings were used, except for mem.mean (set to 0.4) and acc.shape (set to 0.5). Ages are modelled as drawn from

Clim. Past Discuss., doi:10.5194/cp-2016-59, 2016
Manuscript under review for journal Clim. Past
Published: 20 June 2016

a t–distribution, with 9 degrees of freedom (t.a=9, t.b=10). 1,000 age–depth realizations were used to estimate mean age and 95 % confidence intervals at 0.5 cm resolution (Fig. 3).

3.3 Stable carbon isotope analyses

Around 10 tests of *G. ruber* white *sensu stricto* (Wang, 2000) within the size range 250-350 μm and 8 tests of *G. inflata* non–encrusted with 3 chamber in the final whorl (Groeneveld and Chiessi, 2011) within the size range 315-400 μm were hand–picked under a binocular microscope every 2.5 cm from 290 to 768 cm core depth. While the first species records the conditions at the top of the mixed layer (down to ca. 30 m) (Chiessi et al., 2007; Wang, 2000), the second species records the conditions at the permanent thermocline (ca. 350-400 m) (Groeneveld and Chiessi, 2011), allowing the reconstruction of the $\delta^{13}C$ signal of the TW and the SACW, respectively. The $\delta^{13}C$ analyses were performed on a Finnigan MAT 252 mass spectrometer equipped with an automatic carbonate preparation device at the MARUM – Centre for Marine Environmental Sciences, University of Bremen, Germany. Isotopic results are reported in the usual delta–notation relative to the Vienna Peedee belemnite (VPDB). Data were calibrated against the house standard (Solnhofen limestone), itself calibrated against the NBS19 standard. The standard deviation of the laboratory standard was lower than 0.05‰ for the measuring period.

4 Results

4.1 Age model

Our age model covers the period between 32.6 and 5.7 cal ka BP (Table 1, Fig. 3). Sedimentation rates change markedly during this time interval with values ranging from 3.8 to 111 cm ka^{-1}. Three main peaks in sedimentation rate were identified at ca. 26, 23 and 15 and one minor peak at 11 cal ka BP. The two oldest sedimentation peaks occur within our period of interest (i.e., from ca. 33 until 20 cal ka BP), and received special attention due to the higher sedimentation rate which provides increased temporal resolution (Fig. 3). The mean temporal resolution of our $\delta^{13}C$ records is ca. 90 yr with values ranging from 28 and 195 yrs.

4.2 Stable carbon isotopes analyses

The *G. ruber* $\delta^{13}C$ record shows two long–term decreases, from ca. 32.6 to 28.5 cal ka BP with amplitude of ca. 1‰ and from ca. 26.5 to 24.8 cal ka BP also with amplitude of ca. 1‰ (Fig. 4a). These two negative long–term trends are separated from each other by an abrupt increase of ca. 1.3‰ ending at ca. 27 cal ka BP. Both long–term decreasing slopes were interrupted by brief positive excursions, one from 30.6 to 30.4 cal ka BP with amplitude of ca. 0.7‰ and other from ca. 26.2 to 25.8 cal ka BP with amplitude of ca. 1‰. After the second long–term decrease, the $\delta^{13}C$ values of *G. ruber* varied around 0.7‰. Both long–term negative excursions determine a pattern we refer to as "w–structure".

Clim. Past Discuss., doi:10.5194/cp-2016-59, 2016
Manuscript under review for journal Clim. Past
Published: 20 June 2016

Climate of the Past Discussions

The *G. inflata* $\delta^{13}C$ record shows four negative excursions departing from a baseline of ca. 0.8‰ (Fig. 4b). The first occurs from ca. 32.5 to 30.6 cal ka BP with an amplitude of ca. 0.5‰, the second from ca. 29.8 to 28.3 cal ka BP with the same amplitude, the third from ca. 26.5 to 26.4 cal ka BP with an amplitude of ca. 0.8‰, and the forth from ca. 25.8 to 24.4 cal ka BP with an amplitude of ca. 0.9‰. Also in the $\delta^{13}C$ record from *G. inflata* two w–structures are present and are defined by the previously described negative excursions.

The w–structures for both species as well as the $\delta^{13}C$ minima are synchronous (Fig. 4).

5 Discussion

The synchronous w–structures present in the $\delta^{13}C$ records of both planktonic foraminiferal species analysed here occur in consonance with the millennial–scale events HS3 and HS2 (Sarnthein et al., 2001; Goni and Harrison, 2010) (Fig. 4). Based on modern conditions, we expect our core site not to be influenced by significant changes in the nutrient content of the upper water column since the region is dominated by the oligotrophic BC, characteristic of western boundary currents and is far from upwelling cells (Brandini et al., 2000). Thus, it is unlikely that changes in our $\delta^{13}C$ records are associated with local productive events driven by nutrient–cycle processes (Mulitza et al., 1999).

A pervasive feature of planktonic foraminiferal $\delta^{13}C$ records in the Indo–Pacific Ocean (Spero and Lea, 2002), Southern Ocean (Ninnemann and Charles, 1997), and South Atlantic Ocean (Oppo and Fairbanks, 1989) is a negative excursion during HS1. Ninnemann and Charles (1997) suggested that the source for this signal is in the Southern Ocean. They further proposed that the anomaly is related to the transfer of a preformed $\delta^{13}C$ signal from the Southern Ocean via SAMW and/or AAIW. A low–density type of SAMW actually contributes to SACW that spreads into the South Atlantic (Stramma and England, 1999). Additionally, AAIW also influences SACW through vigorous eddy mixing at the Brazil/Malvinas Confluence (Piola and Georgi, 1982). Thus, SACW represents a potential conduit for the $\delta^{13}C$ signal from the sub–Antarctic region to the subtropical South Atlantic (Fig. 1 and 2). Therefore, we propose that the negative excursions in our $\delta^{13}C$ records are related to the transfer of a preformed $\delta^{13}C$ signal from the subantarctic zone to the western South Atlantic via central and thermocline waters.

5.1 Millennial–scale changes: Atlantic Ocean, Southern Ocean and CO_{2atm}

Concomitantly to the periods of low $\delta^{13}C$ in our records a weak AMOC was described based on $^{231}Pa/^{230}Th$ records from the Bermuda Rise (ODP Site 1063, 33.7° N, 57.6° W) (Lippold et al., 2009) that characterize HS3 and HS2 (Fig. 5d). Both events are also marked by pulses of ice-rafted debris (IRD) (MD99-2331, 42.2° N, 9.7° W) (Eynaud et al., 2009) and by decreases in SST (SU8118 and MD952042, 37.5° N, 10.1° W) (Bard, 2002) in the north–eastern North Atlantic (Iberian Margin). The Greenland GISP2 ice core (72.6° N, 38.5° W) shows synchronous increases in Ca^{+2}, indicating changes in atmospheric circulation over Greenland (Mayewski et al., 1997) (Fig. 5a, b, c). It is worth to note that the four records (i.e.,

Clim. Past Discuss., doi:10.5194/cp-2016-59, 2016
Manuscript under review for journal Clim. Past
Published: 20 June 2016

Fig. 5a, b, c, d) mentioned above also show a w–structure during HS2, similar to the one shown in our $\delta^{13}C$ records. The IRD (Eynaud et al., 2009) and Ca^{+2} (Mayewski et al., 1997) records also show a w–structure similar to ours during HS3.

The reduced AMOC would decrease the sub–tropical heat transport towards the north, leading to rising temperatures in the circum–Antarctic region (EDML, 75° S, 0° E, EPICA) (EPICA Community Members, 2006) (Fig. 5i). Furthermore, during phases of weak AMOC the Southern Hemisphere westerlies are stronger and shift southward strengthening CDW upwelling (Anderson et al., 2009; Denton et al., 2010). Increased upwelling would supply the surface of the Southern Ocean to the south of the Antarctic Polar Front with more low–$\delta^{13}C$ waters and with a higher concentration of $Si(OH)_4$ (Anderson et al., 2009; Hendry et al., 2012). Since upwelled CDW is hypothesized to be the dominant source of the upper and intermediate waters that leave the Southern Ocean (i.e., SAMW and AAIW) (Fig. 2), increased upwelling would transfer the low $\delta^{13}C$ signal as well as the positive $Si(OH)_4$ anomaly northward into the adjacent subtropical gyres (Oppo and Fairbanks, 1989; Ninnemann and Charles, 1997; Spero and Lea, 2002; Anderson et al., 2009; Hendry et al., 2012). These signals would then propagate through the thermocline (i.e., SACW) of the South Atlantic, and be transferred to the mixed layer by vertical exchange process (i.e., TW) (Tomczak and Godfrey, 2003). However, we cannot exclude the possibility that the upwelled low–$\delta^{13}C$ respired CO_2 could have been first outgassed from the Southern Ocean, and then re–dissolved into the ocean via air–sea exchanges at the formation regions of SACW and TW, eventually reaching the upper water column at our core site.

Higher concentrations of $Si(OH)_4$ were described in benthic organisms at intermediate water depths (i.e., 1048 m water depths) of the western South Atlantic (ca. 27° S) close to our core site during abrupt millennial–scale climate change events (Hendry et al., 2012), suggesting that the preformed signal from the Southern Ocean indeed reached subtropical latitudes in the South Atlantic.

Millennial–scale changes of the Southern Ocean temperature and deep water ventilation also led to the increase in CO_{2atm} (Spero and Lea, 2002; Ahn and Brook, 2008; Ahn and Brook, 2014; Gottschalk et al., 2015). During HS3 and HS2, positive peaks in CO_{2atm} (Siple Dome, 81.7° S, 148.8° W) (Ahn and Brook, 2014) (Fig. 5k) were described to be synchronous to circum–Antarctic warming (EPICA Community Members, 2006) (Fig. 5i), and most likely have originated from the reduced stratification of the Southern Ocean and consequent release of the remineralized carbon (^{12}C–enriched CO_2) stored for a long period in deep waters (Anderson et al., 2009; Denton et al., 2010; Jaccard et al., 2016; Mariotti et al., 2016). Despite the low temporal resolution, even the $\delta^{13}C$ record of CO_{2atm} at Taylor Dome (77.8° S, 158.7° E) on Antarctica shows a decrease during HS2 (Smith et al., 1999) (Fig. 5j). However, the CO_{2atm} peaks occur ca. 1 ka later than the initiation of the $\delta^{13}C$ decrease in our records. Spero and Lea (2002) also observed a similar offset between the increase in CO_{2atm} and the decrease in Pacific Ocean planktonic foraminifera $\delta^{13}C$ during HS1, and attributed this apparent offset to uncertainties in the age models of their records. An alternative explanation relates to a possible time lag between the weakening of the AMOC and the increase in CO_{2atm} (Ahn and Brook, 2014).

Thus, our records are consistent with the hypothesis that the increase in CO_{2atm} during abrupt millennial–scale climate change events of the last glacial period is originated by ocean processes (Smith et al., 1999; Ahn and Brook, 2008; Bereiter

Clim. Past Discuss., doi:10.5194/cp-2016-59, 2016
Manuscript under review for journal Clim. Past
Published: 20 June 2016

et al., 2012; Ahn and Brook, 2014) and is most likely related to a weak AMOC and associated strengthened Southern Ocean upwelling.

5.2 Continental responses

Paleoclimate records from South America have shown marked hydrological changes during abrupt millennial–scale climate events (Arz et al., 1998; Peterson et al., 2000; Baker et al., 2001; Cruz et al., 2006; Stríkis et al., 2015). Reconstructions of the SAMS activity suggest its strengthening during HSs (Cruz et al., 2006; Kanner et al., 2012; Cheng et al., 2013). Changes in speleothem oxygen isotopic composition from the western Amazon Basin (NAR-C, Cueva del Diamante cave, northern Peru, 5.4° S, 77.3° W) (Cheng et al., 2013) as well as changes on gamma radiation records from the Bolivian Altiplano (Salar de Uyuni, 20.3° S, 67.5° W) (Baker et al., 2001) (Fig. 5f, g) suggest increased precipitation during HS3 and HS2. To the north of the equator, a reflectance record from the Cariaco Basin (off northern Venezuela, MD03-2621, 10.7° N, 65° W) (Deplazes et al., 2013) suggests decreased precipitation during the same millennial–scale events (Fig. 5e). The opposite behaviour of these sites reflects the interhemispheric anti-phase response of tropical precipitation during HSs (Wang et al., 2007; Cheng et al., 2013). Importantly, during HS3 and particularly HS2 the three above mentioned records (Fig. 5e, f, g) show a w–structure similar to the one observed in our $\delta^{13}C$ records. Stríkis et al. (2015) reported a similar w–structure during HS1 related to two distinct hydrologic phases within HS1.

Periods of intensified SAMS would have strengthened the discharge from the Plata River drainage basin (Chiessi et al., 2009), increasing the delivery of terrigenous sediments to the Rio Grande Cone (Lantzsch et al., 2014), our coring site. We show for the first time increased sedimentation rates during a HS off SESA. Thus, the increased sedimentation rates during HS2 in our records corroborate the suggestion of Chiessi et al. (2009). Furthermore, GeoB6212-1 sedimentation rates also show a w–structure during HS2 (Fig. 3), hinting for a sensitive response of the Plata River drainage basin to the increase in activity of the SAMS.

The increased continental runoff that led to increased delivery of terrigenous sediments to our core site could have also enhanced the nutrient availability and the local primary productivity, affecting our planktonic foraminiferal $\delta^{13}C$ records. However, we discard this possibility because the expected signal of stronger local primary productivity on planktonic foraminiferal $\delta^{13}C$ would be opposite to the one observed at GeoB6212-1 (Mulitza et al., 1999).

The occurrence of a similar w–structure in North Atlantic records, in South American records and in our $\delta^{13}C$ and sedimentation rate records gives us confidence that such w–structure is indeed a feature of HS2, and possibly also HS3.

6 Conclusions

Our mixed layer and permanent thermocline $\delta^{13}C$ records from the western South Atlantic show in-phase millennial–scale decreases of up to 1‰ during the HS3 and HS2. We hypothesize that the source of the low $\delta^{13}C$ signal can be explained by millennial–scale changes in the Southern Ocean deep water ventilation. A weak AMOC during HS3 and HS2 would produce

Clim. Past Discuss., doi:10.5194/cp-2016-59, 2016
Manuscript under review for journal Clim. Past
Published: 20 June 2016

stronger Southern Ocean upwelling that in turn, would supply the surface of the Southern Ocean with more low–$\delta^{13}C$ waters as well as promote increased outgassing of this old low–$\delta^{13}C$ respired CO_2. The low–$\delta^{13}C$ waters at the surface of the Southern Ocean would be subducted into the central and thermocline waters and transferred equatorward via the South Atlantic subtropical gyre circulation towards our core site. Together with other lines of evidence, our data are consistent with the hypothesis that the CO_2 added to the atmosphere during abrupt millennial–scale climate change events of the last glacial period originated in the ocean and reached the atmosphere by outgassing of the Southern Ocean. Moreover, the occurrence of a similar w–structure during HS2 (and possibly HS3) in North Atlantic and South American records as well as in our planktonic foraminiferal $\delta^{13}C$ and sedimentation rate records gives us confidence that such w–structure is a pervasive feature that characterizes HS2 (and possibly HS3).

Data availability

The data reported here will be archived in Pangaea (www.pangaea.de).

Acknowledgements

We thank Y. Zhang for help with the Bacon software. Logistic and technical assistance was provided by the captain and crew of the R/V Meteor. M. C. Campos acknowledges the financial support from FAPESP (grants 2013/25518-2 and 2015/11016-0), and C. M. Chiessi acknowledges the financial support from FAPESP (grant 2012/17517-3) and CAPES (grants 1976/2014 and 564/2015). H. Kuhnert, S. Mulitza and I. Voigt were funded through the DFG Research Centre/Cluster of Excellence "The Ocean in the Earth System". A. R. Piola was funded by grant CRN3070 from the Inter-American Institute for Global Change Research through the US National Science Foundation grant GEO-1128040. Sample material was provided by the GeoB Core Repository at the MARUM – Center for Marine Environmental Sciences, University of Bremen, Germany.

References

Ahn, J. and Brook, E. J.: Atmospheric CO_2 and climate on millennial time scales during the last glacial period, Science, 322, 83-85, doi:10.1126/science.1160832, 2008.

Ahn, J. and Brook, E. J.: Siple Dome ice reveals two modes of millennial CO_2 change during the last ice age, Nature Communications, 5, doi:10.1038/ncomms4723, 2014.

Andersen, K. K., Svensson, A., Johnsen, S. J., Rasmussen, S. O., Bigler, M., Rothlisberger, R., Ruth, U., Siggaard-Andersen, M.-L., Steffensen, J. P., Dahl-Jensen, D., Vinther, B. M., and Clausen, H.B.: The Greenland Ice Core Chronology 2005, 15-42 ka. Part 1: constructing the time scale, Quaternary Sci Rev, 25, 3246-3257, doi:10.1016/j.quascirev.2006.08.002, 2006.

Clim. Past Discuss., doi:10.5194/cp-2016-59, 2016
Manuscript under review for journal Clim. Past
Published: 20 June 2016

Anderson, R. F., Ali, S., Bradtmiller, L. I., Nielsen, S. H. H., Fleisher, M. Q., Anderson, B. E., and Burckle, L. H.: Wind-Driven Upwelling in the Southern Ocean and the Deglacial Rise in Atmospheric CO_2, Science, 323, 1443-1448, doi:10.1126/science.1167441, 2009.

Arz, H. W., Pätzold, J., and Wefer, G.: Correlated millennial-scale changes in surface hydrography and terrigenous sediment yield inferred from last-glacial marine deposits off northeastern Brazil, Quaternary Res, 50, 157-166, doi:10.1006/qres.1998.1992, 1998.

Baker, P. A., Rigsby, C. A., Seltzer, G. O., Fritz, S. C., Lowenstein, T. K., Bacher, N. P., and Veliz, C.: Tropical climate changes at millennial and orbital timescales on the Bolivian Altiplano, Nature, 409, 698-701, doi:10.1038/35055524, 2001.

Bard, E.: Correction of accelerator mass spectrometry ^{14}C ages measured in planktonic foraminifera: paleoceanographic implications, Paleoceanography, 3, 635-645, doi:10.1029/PA003i006p00635, 1988.

Bard, E.: Climate shock: Abrupt changes over millennial time scales, Phys Today, 55, 32-38, 2002.

Bard, E., Rostek, F., Turon, J. L., and Gendreau, S.: Hydrological impact of Heinrich events in the subtropical northeast Atlantic, Science, 289, 1321-1324, doi:10.1126/science.289.5483.1321, 2000.

Barker, S., Diz, P., Vautravers, M. J., Pike, J., Knorr, G., Hall, I. R., and Broecker, W. S.: Interhemispheric Atlantic seesaw response during the last deglaciation, Nature, 457, 1097-1102, doi:10.1038/nature07770, 2009.

Berbery, E. H. and Barros, V. R.: The hydrologic cycle of the La Plata basin in South America, J Hydrometeorol, 3, 630-645, doi:10.1175/1525-7541(2002)003<0630:THCOTL>2.0.CO;2, 2002.

Bereiter, B., Luthi, D., Siegrist, M., Schupbach, S., Stocker, T. F., and Fischer, H.: Mode change of millennial CO_2 variability during the last glacial cycle associated with a bipolar marine carbon seesaw, P Natl Acad Sci USA, 109, 9755-9760, doi:10.1073/pnas.1204069109, 2012.

Blaauw, M. and Christen, A. J.: Flexible Paleoclimate Age-Depth Models Using an Autoregressive Gamma Process, Bayesian Analysis, 6, 457-474, doi:10.1214/11-BA618, 2011.

Brandini, F. P., Boltovskoy, D., Piola, A., Kocmur, S., Röttgers, R., Cesar Abreu, P., and Mendes Lopes, R.: Multiannual trends in fronts and distribution of nutrients and chlorophyll in the southwestern Atlantic (30–62° S), Deep-Sea Res Pt I, 47, 1015-1033, doi:10.1016/S0967-0637(99)00075-8, 2000.

Broecker, W. S.: Paleocean circulation during the last deglaciation: A bipolar seesaw? Paleoceanography, 13, 119-121, 1998.

Carvalho, L. M. V., Jones, C., and Liebmann, B.: The South Atlantic convergence zone: Intensity, form, persistence, and relationships with intraseasonal to interannual activity and extreme rainfall, J Climate, 17, 88-109, doi:http://dx.doi.org/10.1175/1520-0442(2004)017<0088:TSACZI>2.0.CO;2, 2004.

Charles, C. D. and Fairbanks, R. G.: Evidence from Southern-Ocean sediments for the effect of North-Atlantic Deep-Water flux on climate, Nature, 355, 416-419, doi:10.1038/355416a0, 1992.

Chaves, R. R. and Nobre, P.: Interactions between sea surface temperature over the South Atlantic Ocean and the South Atlantic Convergence Zone, Geophys Res Lett, 31, doi:10.1029/2003GL018647, 2004.

Cheng, H., Sinha, A., Cruz, F. W., Wang, X., Edwards, R. L. A., d'Horta, F. M., Ribas, C. C., Vuille, M., Stott, L. D., and Auler, A. S.: Climate change patterns in Amazonia and biodiversity, Nature Communications, 4, doi:10.1038/ncomms2415, 2013.

Chiessi, C. M., Ulrich, S., Mulitza, S., Paetzold, J., and Wefer, G.: Signature of the Brazil-Malvinas Confluence (Argentine Basin) in the isotopic composition of planktonic foraminifera from surface sediments, Mar Micropaleontol, 64, 52-66, doi:10.1016/j.marmicro.2007.02.002, 2007.

Chiessi, C. M., Mulitza, S., Paetzold, J., Wefer, G., and Marengo, J. A.: Possible impact of the Atlantic Multidecadal Oscillation on the South American summer monsoon, Geophys Res Lett, 36, L21707, doi:10.1029/2009GL039914, 2009.

Chiessi, C. M., Mulitza, S., Mollenhauer, G., Silva, J. B., Groeneveld, J., and Prange, M.: Thermal evolution of the western South Atlantic and the adjacent continent during Termination 1, Clim Past, 11, 915-929, doi:10.5194/cp-11-915-2015, 2015.

Crowley, T. J.: North Atlantic Deep Water cools the Southern Hemisphere, Paleoceanography, 7, 489-497, doi:10.1029/92PA01058 1992.

Cruz, F. W., Jr., Burns, S. J., Karmann, I., Sharp, W. D., and Vuille, M.: Reconstruction of regional atmospheric circulation features during the late Pleistocene in subtropical Brazil from oxygen isotope composition of speleothems, Earth Planet Sc Lett, 248, 495-507, doi:10.1016/j.epsl.2006.06.019, 2006.

Denton, G. H., Anderson, R. F., Toggweiler, J. R., Edwards, R. L., Schaefer, J. M., and Putnam, A. E.: The Last Glacial Termination, Science, 328, 1652-1656, doi:10.1126/science.1184119 2010.

Deplazes, G., Lueckge, A., Peterson, L. C., Timmermann, A., Hamann, Y., Hughen, K. A., Roehl, U., Laj, C., Cane, M. A., Sigman, D. M., and Haug, G. H.: Links between tropical rainfall and North Atlantic climate during the last glacial period, Nat Geosci, 6, 213-217, doi:10.1038/ngeo1712, 2013.

EPICA Community Members: One-to-one coupling of glacial climate variability in Greenland and Antarctica, Nature, 444, 195-198, doi:10.1038/nature05301, 2006.

Eynaud, F., de Abreu, L., Voelker, A., Schoenfeld, J., Salgueiro, E., Turon, J.-L., Penaud, A., Toucanne, S., Naughton, F., Goni, M. F. S., Malaize, B., and Cacho, I.: Position of the Polar Front along the western Iberian margin during key cold episodes of the last 45 ka, Geochem Geophy Geosy, 10, doi:10.1029/2009GC002398, 2009.

Garcia, H. E., Locarnini, R. A., Boyer, T. P., Antonov, J. I., Baranova, O. K., Zweng, M. M., Reagan, J. R., and Johnson, D. R.: World Ocean Atlas 2013, Volume 4: Dissolved Inorganic Nutrients (phosphate, nitrate, silicate), in: Levitus, S., Mishonov, A. (Eds.). NOAA Atlas NESDIS, p. 25, 2014.

Garreaud, R. D., Vuille, M., Compagnucci, R., and Marengo, J.: Present-day South American climate, Palaeogeogr Palaeocl, 281, 180-195, doi:10.1016/j.palaeo.2007.10.032, 2009.

Goni, M. F. S. and Harrison, S. P.: Millennial-scale climate variability and vegetation changes during the Last Glacial: Concepts and terminology Introduction, Quaternary Sci Rev, 29, 2823-2827, doi:10.1016/j.quascirev.2009.11.014, 2010.

Gordon, A. L.: South-Atlantic thermocline ventilation, Deep-Sea Res, 28, 1239-1264, doi:10.1016/0198-0149(81)90033-9, 1981.

Gottschalk, J., Skinner, L. C., and Waelbroeck, C.: Contribution of seasonal sub-Antarctic surface water variability to millennial-scale changes in atmospheric CO_2 over the last deglaciation and Marine Isotope Stage 3, Earth Planet Sc Lett, 411, 87-99, doi:10.1016/j.epsl.2014.11.051, 2015.

Groeneveld, J. and Chiessi, C. M.: Mg/Ca of Globorotalia inflata as a recorder of permanent thermocline temperatures in the South Atlantic, Paleoceanography, 26, doi:10.1029/2010pa001940, 2011.

Hendry, K. R., Robinson, L. F., Meredith, M. P., Mulitza, S., Chiessi, C. M., and Arz, H.: Abrupt changes in high-latitude nutrient supply to the Atlantic during the last glacial cycle, Geology, 40, 123-126, doi:10.1130/G32779.1, 2012.

Jaccard, S. L., Galbraith, E. D., Martínez-García, A., and Anderson, R. F.: Covariation of deep Southern Ocean oxygenation and atmospheric CO_2 through the last ice age, Nature, 530, 207-210, doi:10.1038/nature16514, 2016.

Kanner, L. C., Burns, S. J., Cheng, H., and Edwards, R. L.: High-Latitude Forcing of the South American Summer Monsoon During the Last Glacial, Science, 335, 570-573, doi:10.1126/science.1213397, 2012.

Knight, J. R., Allan, R. J., Folland, C. K., Vellinga, M., and Mann, M. E.: A signature of persistent natural thermohaline circulation cycles in observed climate, Geophys Res Lett, 32, L20708, doi:10.1029/2005GL024233, 2005.

Kroopnick, P. M.: The distribuction of C-13 of sigma-CO_2 in the world oceans, Deep-Sea Res, 32, 57-84, doi:10.1016/0198-0149(85)90017-2, 1985.

Lantzsch, H., Hanebuth, T. J. J., Chiessi, C. M., Schwenk, T., and Violante, R. A.: The high-supply, current-dominated continental margin of southeastern South America during the late Quaternary, Quaternary Res, 81, 339-354, doi:10.1016/j.yqres.2014.01.003, 2014.

Lippold, J., Gruetzner, J., Winter, D., Lahaye, Y., Mangini, A., and Christl, M.: Does sedimentary $^{231}Pa/^{230}Th$ from the Bermuda Rise monitor past Atlantic Meridional Overturning Circulation? Geophys Res Lett, 36, doi:10.1029/2009GL038068, 2009.

Locarnini, R. A., Mishonov, A. V., Antonov, J. I., Boyer, T. P., Garcia, H. E., Baranova, O. K., Zweng, M. M., Paver, C. R., Reagan, J. R., Johnson, D. R., Hamilton, M., and Seidov, D.: World Ocean Atlas 2013, Volume 1: Temperature, in: Levitus, S., Mishonov, A. (Eds.). NOAA Atlas NESDIS, p. 40, 2013.

Mariotti, V., Paillard, D., Bopp, L., Roche, D. M., and Bouttes, N.: A coupled model for carbon and radiocarbon evolution during the last deglaciation, Geophys Res Lett, 43, doi:10.1002/2015GL067489, 2016.

Marshall, J. and Speer, K.: Closure of the meridional overturning circulation through Southern Ocean upwelling, Nat Geosci, 5, 171-180, doi:10.1038/ngeo1391, 2012.

Mayewski, P. A., Meeker, L. D., Twickler, M. S., Whitlow, S., Yang, Q. Z., Lyons, W. B., and Prentice, M.: Major features and forcing of high-latitude northern hemisphere atmospheric circulation using a 110,000-year-long glaciochemical series, J Geophys Res-Oceans, 102, 26345-26366, doi:10.1029/96JC03365, 1997.

McCartney, M. S.: Subantarctic Mode Water, in: Angel, M.V. (Ed.), A Voyage of Discovery. Oxford, 1977.

Mémery, L., Arhan, M., Alvarez-Salgado, X. A., Messias, M. J., Mercier, H., Castro, C. G., and Rios, A. F.: The water masses along the western boundary of the south and equatorial Atlantic, Prog Oceanogr, 47, 69-98, doi:10.1016/S0079-6611(00)00032-X, 2000.

Mix, A. C., Ruddiman, W. F., and McIntyre, A.: Late Quaternary paleoceanography of the Tropical Atlantic, 1: spatial variability of annual mean sea-surface temperatures, 0-20,000 years BP, Paleoceanography, 1, 43-66, 10.1029/PA001i001p00043, 1986.

Molinelli, E. J.: The Antarctic influence on Antarctic Intermediate Water, J Mar Res, 39, 267-293, 1981.

Mulitza, S., Arz, H., Mücke, S. K., Moos, C., Niebler, H. -S., Pätzold, J., and Segl, M.: The South Atlantic Carbon Isotope Record of Planktic Foraminifera, in: Fischer, G., Wefer, G. (Eds.), Use of Proxies in Paleoceanography: Examples from South Atlantic. Springer-Verlag, Berlin Heidelberg, pp. 427-445, 1999.

Naveira Garabato, A. C. N., Jullion, L., Stevens, D. P., Heywood, K. J., and King, B. A.: Variability of Subantarctic Mode Water and Antarctic Intermediate Water in the Drake Passage during the Late-Twentieth and Early-Twenty-First Centuries, J Climate, 22, 3661-3688, doi:http://dx.doi.org/10.1175/2009JCLI2621.1, 2009.

Ninnemann, U. S. and Charles, C. D.: Regional differences in Quaternary Subantarctic nutrient cycling: Link to intermediate and deep water ventilation, Paleoceanography, 12, 560-567, doi:10.1029/97PA01032, 1997.

Olson, D. B., Podesta, G. P., Evans, R. H., and Brown, O. B.: Temporal variations in the separation of Brazil and Malvinas currents, Deep-Sea Res, 35, 1971-1990, doi:10.1016/0198-0149(88)90120-3, 1988.

Oppo, D. W. and Fairbanks, R. G.: Variability in the deep and intermediate water circulation of the Atlantic-Ocean during the past 25,000 years - Northern-Hemisphere modulation of the Southern-Ocean, Earth Planet Sc Lett, 86, 1-15, doi:10.1016/0012-821X(87)90183-X, 1987.

Oppo, D. W. and Fairbanks, R. G.: Carbon isotope composition of tropical surface water during the past 22,000 years, Paleoceanography, 4, 333-351, doi:10.1029/PA004i004p00333, 1989.

Peterson, L. C., Haug, G. H., Hughen, K. A., and Rohl, U.: Rapid changes in the hydrologic cycle of the tropical Atlantic during the last glacial, Science, 290, 1947-1951, doi:10.1126/science.290.5498.1947, 2000.

Peterson, R. G. and Stramma, L.: Upper-level circulation in the South-Atlantic Ocean, Prog Oceanogr, 26, 1-73, 1991.

Piola, A. R. and Georgi, D. T.: Circumpolar properties of Antarctic Intermediate Water and Sub-antarctic Mode Water, Deep-Sea Res, 29, 687-711, doi:10.1016/0198-0149(82)90002-4, 1982.

Piola, A. R. and Gordon, A. L.: Intermediate waters in the southwest South-Atlantic, Deep-Sea Res, 36, 1-16, doi:10.1016/0198-0149(89)90015-0, 1989.

Rasmussen, S. O., Andersen, K. K., Svensson, A. M., Steffensen, J. P., Vinther, B. M., Clausen, H. B., Siggaard-Andersen, M. L., Johnsen, S. J., Larsen, L. B., Dahl-Jensen, D., Bigler, M., Rothlisberger, R., Fischer, H., Goto-Azuma, K., Hansson, M. E., and Ruth, U.: A new Greenland ice core chronology for the last glacial termination, J Geophys Res-Atmos, 111, D06102, doi:10.1029/2005jd006079, 2006.

Reimer, P. J., Bard, E., Bayliss, A., Beck, J. W., Blackwell, P. G., Ramsey, C. B., Buck, C. E., Cheng, H., Edwards, R. L., Friedrich, M., Grootes, P. M., Guilderson, T. P., Haflidason, H., Hajdas, I., Hatte, C., Heaton, T. J., Hoffmann, D. L., Hogg, A. G., Hughen, K. A., Kaiser, K. F., Kromer, B., Manning, S. W., Niu, M., Reimer, R. W., Richards, D. A., Scott, E. M., Southon, J. R., Staff, R. A., Turney, C. S. M., and van der Plicht, J.: IntCal13 and Marine13 radiocarbon age calibration curves 0-50,000 years cal BP, Radiocarbon, 55, 1869-1887, doi:10.2458/azu_js_rc.55.16947, 2013.

Sachs, J. P. and Lehman, S. J.: Subtropical North Atlantic temperatures 60,000 to 30,000 years ago, Science, 286, 756-759, doi:10.1126/science.286.5440.756, 1999.

Sarnthein, M., Stattegger, K., Dreger, D., Erlenkeuser, H., Grootes, P., Haupt, B. J., Jung, S., Kiefer, T., Kuhnt, W., Pflaumann, U., Schafer-Neth, C., Schulz, H., Schulz, M., Seidov, D., Simstich, J., van Kreveld, S., Vogelsang, E., Volker, A., and Weinelt, M.: Fundamental modes and abrupt changes in north Atlantic circulation and climate over the last 60 ky - Concepts, reconstruction and numerical modeling in: The Northern North Atlantic: A Changing Environment, edited by: Schäfer, P., Ritzrau, W., Schlüter, M., and Thiede, J., Springer, Berlin, 365–410, 2001.

Schneider, T., Bischoff, T., Haug, G. H.: Migrations and dynamics of the intertropical convergence zone, Nature, 513, 45-53, doi:10.1038/nature13636, 2014.

Schulz, H. D., Ayres Neto, A., Boetius, A., Enneking, K., Fabian, K., Feseker, T., Funk, J., Gorke, M., Heidersdorf, F., Hensen, C., Heuer, V., Hill, H. G., Hinrichs, S., Kasten, S., Klann, M., Lacerda de Souza, C., Martinez Briao, A., Meyer, S., Mulitza, S., Niebler, H.-S., Ochsenhirt, W.-T., Panteleit, B., Pfeifer, K., Schewe, F., Schwenk, T., Senorans, J. L., Siemer, S., Steinmetz, E., and Wenzhöfer, F.: Report and preliminary results of Meteor Cruise M46/2, Recife (Brazil) – Montevideo (Uruguay), 2 December – 29 December 1999, Fachbereich Geowissenschaften, Universität Bremen, Bremen, 107 pp., 2001.

Smith, H. J., Fischer, H., Wahlen, M., Mastroianni, D., Deck, B.: Dual modes of the carbon cycle since the Last Glacial Maximum, Nature, 400, 248-250, doi:10.1038/22291, 1999.

Spero, H. J.: Do planktic foraminifera accurately record shifts in the carbon isotopic composition of seawater sigma-CO_2? Mar Micropaleontol, 19, 275-285, doi:10.1016/0377-8398(92)90033-G, 1992.

Spero, H. J. and Lea, D. W.: The cause of carbon isotope minimum events on glacial terminations, Science, 296, 522-525, doi:10.1126/science.1069401, 2002.

Sprintall, J. and Tomczak, M.: On the formation of central water and thermocline ventilation in the Southern-Hemisphere, Deep-Sea Res Pt I, 40, 827-848, doi:10.1016/0967-0637(93)90074-D, 1993.

Stocker, T. F. Climate change - The seesaw effect, Science, 282, 61-62, 1998.

Stramma, L. and England, M. H.: On the water masses and mean circulation of the South Atlantic Ocean, J Geophys Res-Oceans, 104, 20863-20883, doi:10.1029/1999JC900139, 1999.

Stramma, L., Ikeda, Y., and Peterson, R. G.: Geostrophic transport in the Brazil Current region north of 20-degrees-S, Deep-Sea Res, 37, 1875-1886, doi:10.1016/0198-0149(90)90083-8, 1990.

Stramma, L., Fischer, J., Brandt, P., and Schott, F.: Circulation, variability and near-equatorial meridional flow in the central tropical Atlantic, Elsev Oceanogr Serie, 68, 1-22, doi:10.1016/S0422-9894(03)80141-1, 2003.

Stríkis, N. M., Chiessi, C. M., Cruz, F. W., Vuille, M., Cheng, H., de Souza Barreto, E. A., Mollenhauer, G., Kasten, S., Karmann, I., Edwards, R. L., Pablo Bernal, J., and Sales, H. D. R.: Timing and structure of Mega-SACZ events during Heinrich Stadial 1, Geophys Res Lett, 42, 5477-5484, doi:10.1002/2015GL064048, 2015.

Svensson, A., Andersen, K. K., Bigler, M., Clausen, H. B., Dahl-Jensen, D., Davies, S. M., Johnsen, S. J., Muscheler, R., Parrenin, F., Rasmussen, S. O., Roethlisberger, R., Seierstad, I., Steffensen, J. P., and Vinther, B. M.: A 60 000 year Greenland stratigraphic ice core chronology, Clim Past, 4, 47-57, 2008.

Talley, L. D.: Closure of the Global Overturning Circulation Through the Indian, Pacific, and Southern Oceans: Schematics and Transports, Oceanography, 26, 80-97, 2013.

Tomczak, M. and Godfrey, J. S.: Regional Oceanography: An Introduction, 2nd ed. Daya Publishing House, Delhi, 2003.

Tomczak, M. and Liefrink, S.: Interannual variations of water mass volumes in the Southern Ocean, Journal of Atmospheric and Ocean Science, 10, doi:10.1080/17417530500062838, 2005.

Tsuchiya, M., Talley, L. D., and McCartney, M. S.: Water-mass distributions in the western South-Atlantic - a section from South Georgia Island (54S) northward across the equator, J Mar Res, 52, 55-81, doi:http://dx.doi.org/10.1357/0022240943076759, 1994.

Wang, L. J.: Isotopic signals in two morphotypes of Globigerinoides ruber (white) from the South China Sea: implications for monsoon climate change during the last glacial cycle, Palaeogeogr Palaeocl, 161, 381-394, doi:10.1016/S0031-0182(00)00094-8, 2000.

Wang, X., Auler, A. S., Edwards, R. L., Cheng, H., Ito, E., Wang, Y., Kong, X., and Solheid, M.: Millennial-scale precipitation changes in southern Brazil over the past 90,000 years, Geophys Res Lett, 34, doi:10.1029/2007GL031149, 2007.

Wefer, G., Adegbie, A. T., Böckel, B., Brauner, R., Büttner, U., Diekamp, V., Dillon, M., Dobeneck, T. v., Donner, B., Eberwein, A., Heinecke-Herzog, M., Kim, J. H., Meier, S., Mollenhauer, G., Olguin, H., Romero, O., Schewe, F., Schlemm, V., Schmieder, F., Schünemann, H., Streng, M., and Volbers, A. N. A.: Report and preliminary results of Meteor Cruise M46/4, Mar del Plata (Argentina) – Salvador da Bahia (Brazil), 10 February – 13 March 2000, With partial results of Meteor Cruise M46/2., Fachbereich Geowissenschaften, Universität Bremen, Bremen, 136 pp., 2001.

Zhou, J. Y. and Lau, K. M.: Does a monsoon climate exist over South America? J Climate, 11, 1020-1040, doi:http://dx.doi.org/10.1175/1520-0442(1998)011<1020:DAMCEO>2.0.CO;2, 1998.

Clim. Past Discuss., doi:10.5194/cp-2016-59, 2016
Manuscript under review for journal Clim. Past
Published: 20 June 2016

Climate of the Past Discussions
Open Access
EGU

Table 1: Accelerator mass spectrometer radiocarbon dates and calibrated ages used to construct the age model of core GeoB6212-1.

Core depth (cm)	Lab ID	Species	Radiocarbon age ± 1σ error (a BP)	Calibrated ages (cal a BP)
8	Poz-47236*	*G. ruber*	5250 ± 40	5694
33	382580**	*G. ruber*	9440 ± 40	10112
58	Poz-47237*	*G. ruber*	10250 ± 50	11345
113	382581**	Planktonic forams	12870 ± 50	14374
158	Poz-47238*	Planktonic forams	13050 ± 70	15179
253	382582**	Planktonic forams	15750 ± 50	18616
323	382583**	Planktonic forams	17560 ± 60	20731
363	Poz-47239*	Planktonic forams	18610 ± 140	21843
478	382584**	Planktonic forams	19810 ± 70	23511
578	Poz-47240*	Planktonic forams	21750 ± 150	25583
623	382585**	Planktonic forams	22320 ± 80	26164
668	382586**	Planktonic forams	22480 ± 80	26645
717	424077**	Planktonic forams	24190 ± 110	27894
768	382587**	Planktonic forams	29520 ± 160	32583

*** Poz: Poznan Radiocarbon Laboratory, Poznan, Poland.**
**** Beta Analytic Radiocarbon Dating Laboratory, Miami, USA.**

Clim. Past Discuss., doi:10.5194/cp-2016-59, 2016
Manuscript under review for journal Clim. Past
Published: 20 June 2016

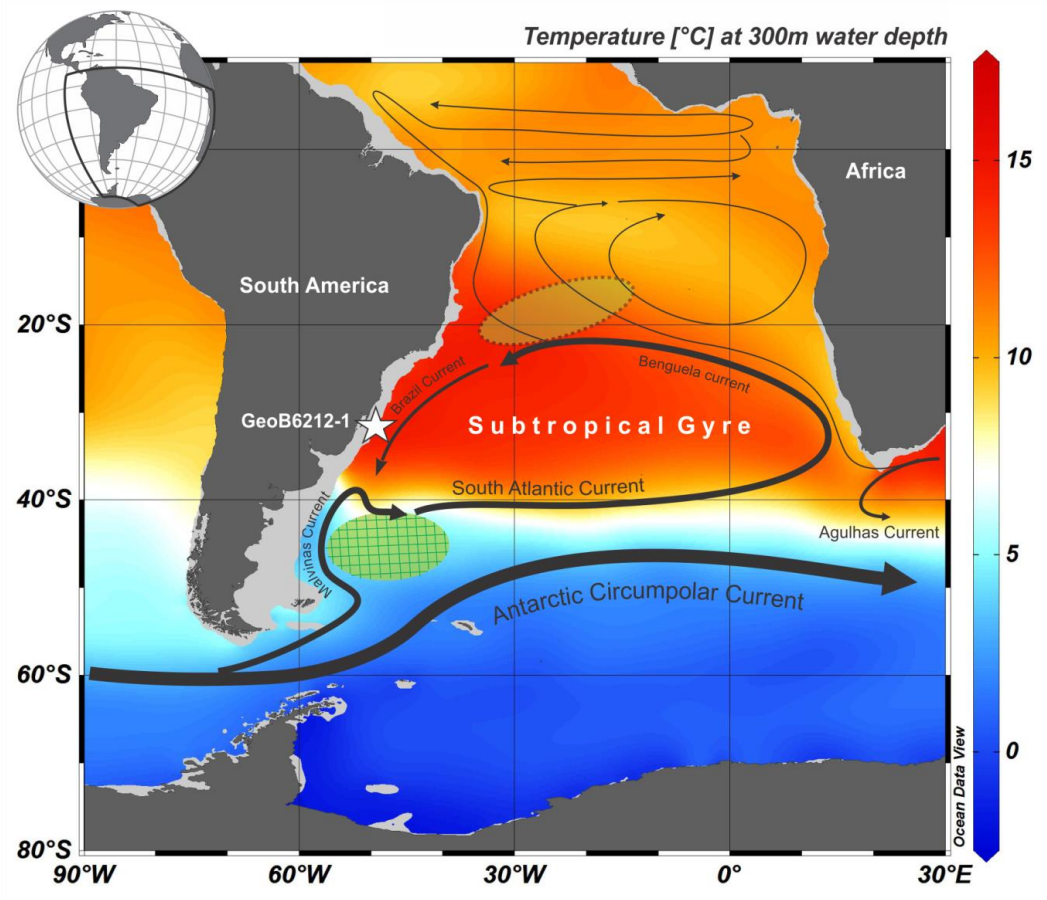

Figure 1: Schematic representation of the large–scale circulation of South Atlantic Central Water (SACW) (Stramma and England, 1999). The main SACW source region is depicted by the gridded green ellipse, and the main source region of tropical subsurface water (TW) is indicated by the dotted yellow ellipse. Mean annual temperature at 300 m water depth is shown by the colour shading (Locarnini et al., 2013).

Clim. Past Discuss., doi:10.5194/cp-2016-59, 2016
Manuscript under review for journal Clim. Past
Published: 20 June 2016

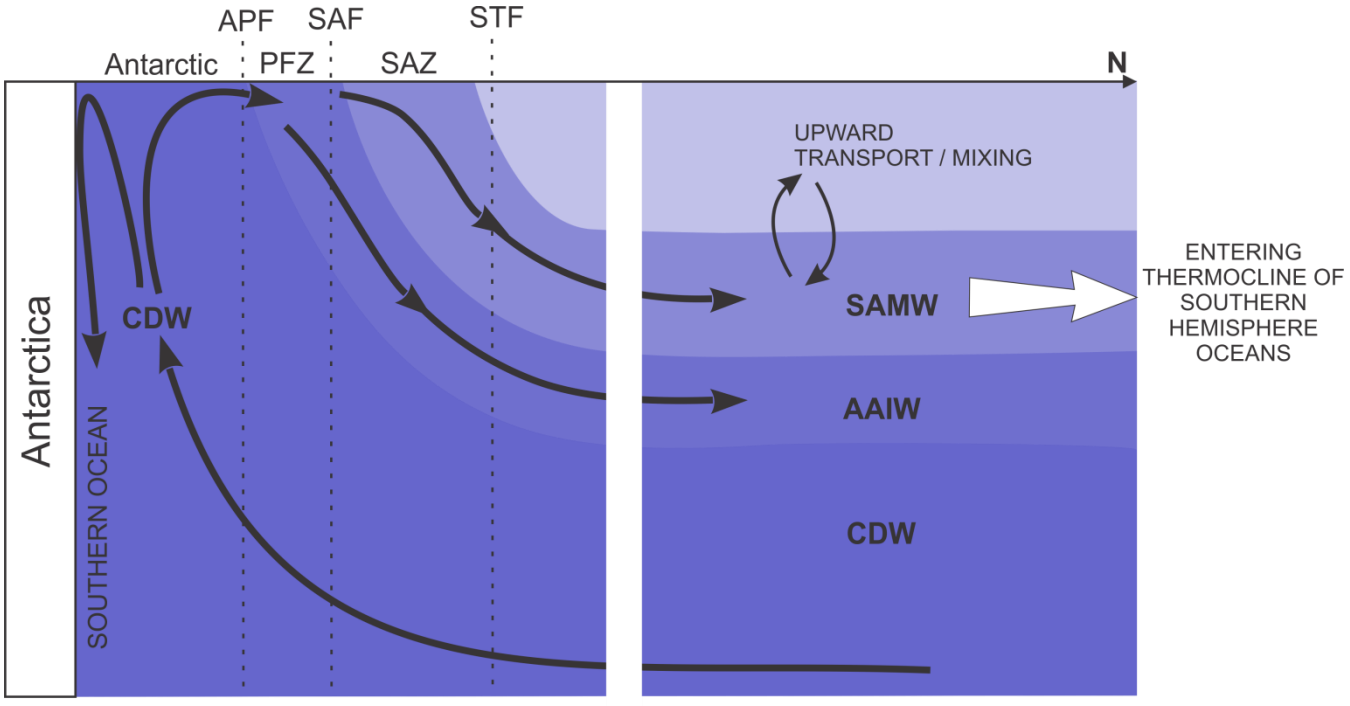

Figure 2: Schematic representation of ventilation and subduction of water masses in the Southern Ocean (modified after Anderson et al., 2009). Wind–driven upwelling south of the latitude of maximum westerlies brings Circumpolar Deep Water (CDW) to the surface and contributes to Antarctic Surface Waters. Antarctic Surface Waters represent the dominant source of the upper and intermediate waters that leave the Southern Ocean. Antarctic Intermediate Water (AAIW) originates by subduction of cold and fresh Antarctic Surface Waters across the Antarctic Polar Front (APF) and enters the South Atlantic mainly via the subtropical gyre. Subantarctic Mode Water (SAMW) originates from deep winter convection north of the Subantarctic Front (SAF). A low–density type of SAMW enters the thermocline of the Southern Hemisphere oceans along the southern edge of the subtropical gyres where it becomes part of central waters and contributes to ventilating the thermocline, while a denser type of SAMW formed in the eastern South Pacific is regarded as a precursor of the AAIW. The Polar Front Zone (PFZ) and Subantarctic Zone (SAZ) are the regions between the APF and SAF, and between the SAF and Subtropical Front (STF), respectively.

Clim. Past Discuss., doi:10.5194/cp-2016-59, 2016
Manuscript under review for journal Clim. Past
Published: 20 June 2016

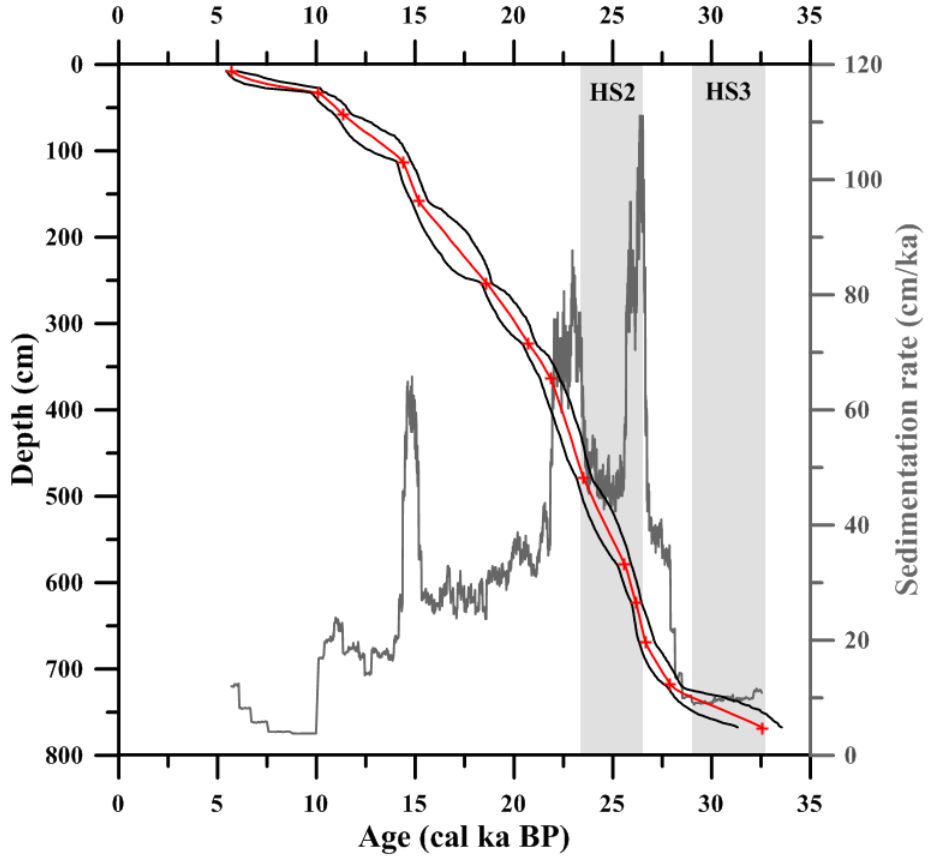

Figure 3: Age model (left hand side y–axis; red line and black enveloping curves) and sedimentation rates (right hand side y–axis; grey line) for marine sediment core GeoB6212-1 produced with the software Bacon 2.2 (Blaauw and Christen, 2011). For the age model, the red symbols show calibrated ages, the red line depicts mean ages and the upper (lower) black line depicts maximum (minimum) ages. Grey vertical bars show abrupt millennial–scale climate change events Heinrich Stadial 3 (HS3) and Heinrich Stadial 2 (HS2) (Goni and Harrison, 2010; Sarnthein et al., 2001).

Clim. Past Discuss., doi:10.5194/cp-2016-59, 2016
Manuscript under review for journal Clim. Past
Published: 20 June 2016

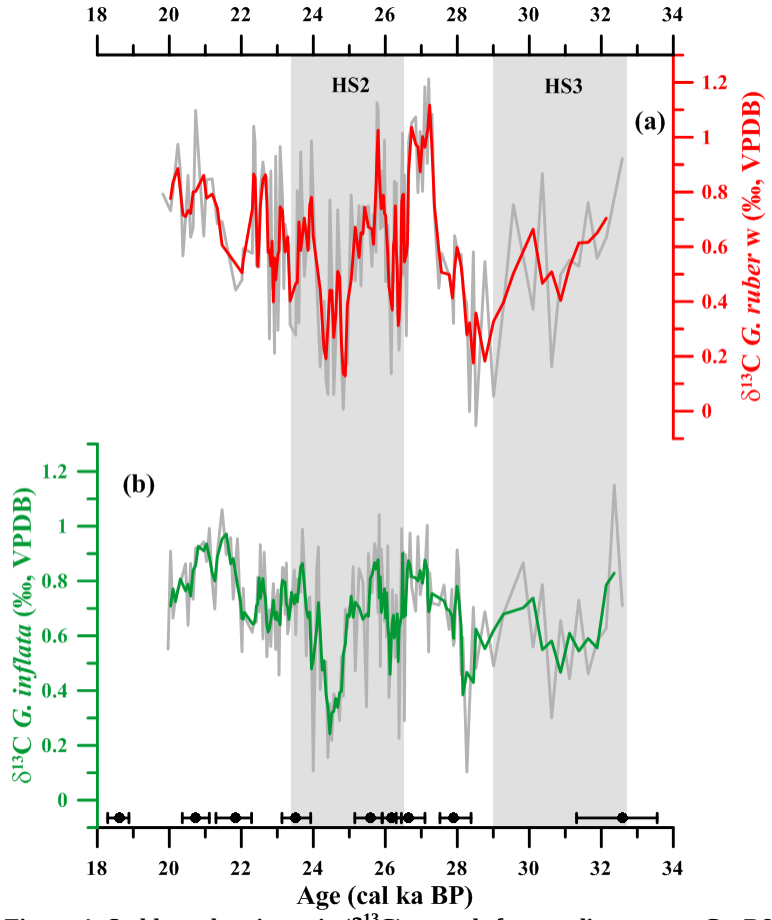

Figure 4: Stable carbon isotopic ($\delta^{13}C$) records from sediment core GeoB6212-1. (a) *Globigerinoides ruber* white (*G. ruber* w) $\delta^{13}C$ and (b) *Globorotalia inflata* (*G. inflata*) $\delta^{13}C$. Red and green lines represent three–point running averages for *G. ruber* and *G. inflata*, respectively. Black symbols at the bottom of the panel depict calibrated ages. Grey vertical bars show abrupt millennial–scale climate change events Heinrich Stadial 3 (HS3) and Heinrich Stadial 2 (HS2) (Goni and Harrison, 2010; Sarnthein et al., 2001).

Clim. Past Discuss., doi:10.5194/cp-2016-59, 2016
Manuscript under review for journal Clim. Past
Published: 20 June 2016

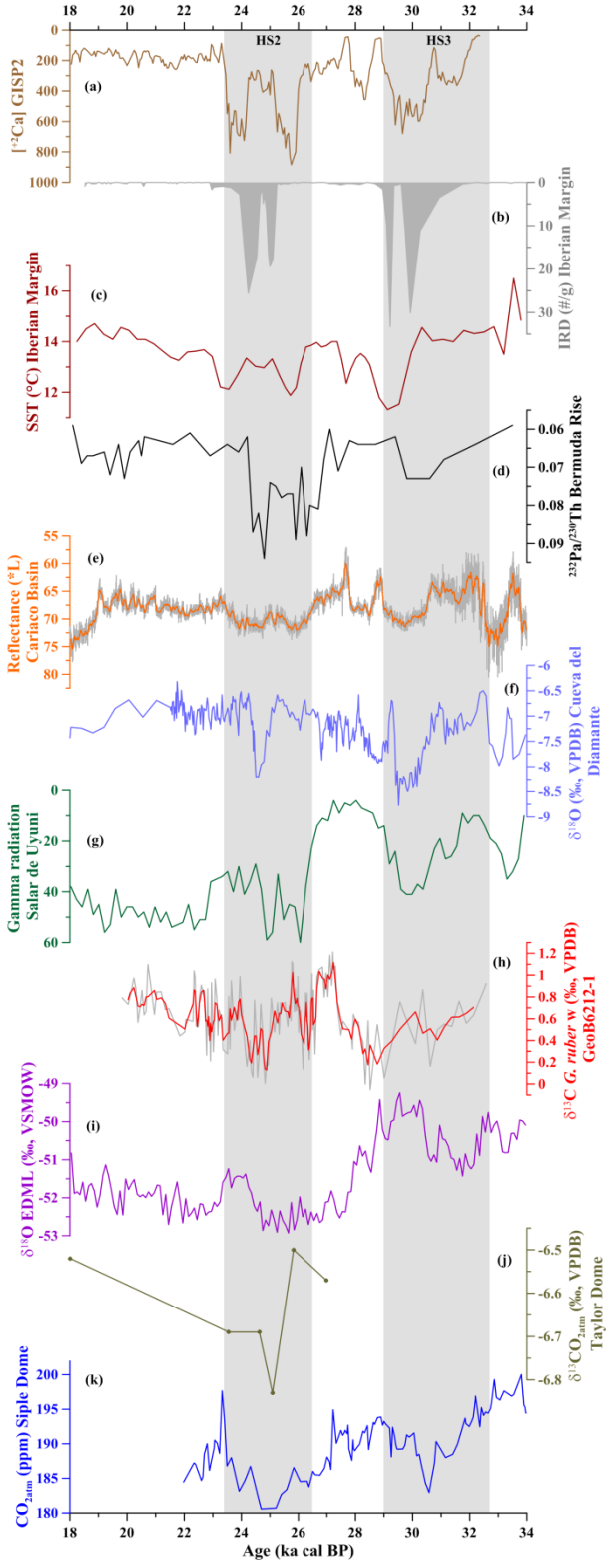

Clim. Past Discuss., doi:10.5194/cp-2016-59, 2016
Manuscript under review for journal Clim. Past
Published: 20 June 2016

Climate of the Past Discussions
Open Access
EGU

Figure 5: Proxy records from the western South Atlantic, western and eastern North Atlantic and tropical South America spanning Heinrich Stadial 3 (HS3) and Heinrich Stadial 2 (HS2) (Goni and Harrison, 2010; Sarnthein et al., 2001). (a) Changes in atmospheric circulation over Greenland derived from Greenland Ice Sheet Project 2 (GISP2) Ca^{+2} concentration (Mayewski et al., 1997) plotted versus the Greenland Ice Core Chronology 2005 (GICC05) (Andersen et al., 2006; Rasmussen et al., 2006) at 72.6° N, 38.5° W; (b) Heinrich layers indicated by the presence of ice-rafted debris (IRD) from the Iberian Margin marine sediment core MD99-2331 at 42.2° N, 9.7° W (Eynaud et al., 2009); (c) sea surface temperature (SST) (°C) changes from Iberian Margin marine sediment cores SU8118 and MD952042 at 37.5° N, 10.1° W (Bard, 2002); (d) Atlantic meridional overturning circulation (AMOC) strength derived from Bermuda Rise sedimentary $^{231}Pa/^{230}Th$ ratio – ODP Site 1063 (higher values indicate a reduced AMOC) at 33.7° N, 57.6° W (Lippold et al., 2009); (e) position of the Intertropical Convergence Zone (ITCZ) indicated by reflectance (*L) (higher values indicate decreased precipitation) from the Cariaco Basin marine sediment core MD03-2621 at 10.7° N, 65° W (Deplazes et al., 2013) (orange line represents a 399-point running average); (f) strength of western Amazon precipitation indicated by the $\delta^{18}O$ from stalagmite NAR-C collected in the Cueva del Diamante Cave, western Amazon (more negative values indicate increased precipitation) at 5.4° S, 77.3° W (Cheng et al., 2013); (g) presence of paleolakes indicated by the natural gamma radiation from Bolivian Altiplano Salar de Uyuni (higher values indicate increased precipitation) at 20.3° S, 67.5° W (Baker et al., 2001); (h) Globigerinoides ruber white (*G. ruber* w) $\delta^{13}C$ from marine sediment core GeoB6212-1 collected in the western South Atlantic at 32.4° S, 50.1° W (red line represents a three–point running average) (this study); (i) atmospheric temperature over Antarctica indicated by EPICA Dronning Maud Land (EPICA Community Members, 2006) $\delta^{18}O$ (higher values indicate warmer conditions) plotted versus its original chronology at 75° S, 0° E; (j) $\delta^{13}C$ of atmospheric CO_2 ($\delta^{13}CO_{2atm}$) from Taylor Dome (lower values indicate increased input to the atmosphere of $\delta^{13}C$–depleted respired CO_2) at 77.8° S, 158.7° E (Smith et al., 1999); (k) atmospheric CO_2 concentration (ppm) from ice core Siple Dome (Ahn and Brook, 2014) plotted versus the Greenland Ice Core Chronology 2005 (GICC05) (Svensson et al., 2008) at 81.7° S, 148.8° W.